

UV and visible absorption in LiTaO₃

Alexei L. Alexandrovski^{*a}, Gisele Foulon^a, Lawrence E. Myers^b, Roger K. Route^a, Martin M. Fejer^a

^aE.L.Ginzton Laboratory, Stanford University, Stanford CA 94305-4085

^bLightwave Electronics Corp., Mountain View, CA

ABSTRACT

The effects of reduction, oxidation, Li-enrichment and impurity on LiTaO₃ crystals are studied. It is demonstrated that the best LiTaO₃ crystals show less absorption than LiNbO₃, less photorefractive damage and no green-light-induced infrared absorption.

Keywords: Lithium tantalate, absorption, UV, visible, defects, LiTaO₃

1. INTRODUCTION

Interest in LiTaO₃ as a material for UV and visible generation has increased recently because its absorption edge extends farther into the UV and it shows less sensitivity to photorefractive damage than LiNbO₃. Moreover, it has been demonstrated¹ that periodically poled LiTaO₃ can be processed with shorter periods than has been possible in LiNbO₃, and hence it is a better candidate for UV generation in a quasi phase-matching configuration.

However, LiTaO₃ usually exhibits an absorption band in the UV with a tail extending up to 400 nm and, although low, its absorption in the blue-green and infrared can be a problem for high power generation. One effect that may severely increase the thermal loading of a crystal against that calculated from linear absorption data is green-light-induced IR absorption (GRIIRA) which is found also in lithium niobate and periodically-poled lithium niobate.²

The aim of this study was to investigate the defects possibly responsible for these absorption phenomena and to find ways to reduce the absorption. Several experiments on oxidation, reduction and lithium enrichment using the vapor transport equilibration³ (VTE) process have been performed. While the absorption near the UV edge could be characterized using traditional spectrophotometry, that in the transparency range of LiTaO₃, including GRIIRA, could only be measured using a more sensitive technique. In response to this need photothermal common-path interferometry (PCI),⁴ a novel modification of the well-known thermal lensing technique⁵ was developed.

2. EXPERIMENTAL

Crystals of LiTaO₃ were provided by several different vendors as either 1 cm³ cubes or 0.5 mm thick wafers. Oxidation experiments were performed at 600°C under oxygen atmospheric pressure for one hour in a tube furnace. Reduction experiments were performed under a mixture of H₂ / N₂ (5% / 95%) at 1000°C.

The procedure for VTE experiments was the following: a wafer of “congruent” composition was placed in a platinum crucible over a mixture of Li₃TaO₄ and LiTaO₃ and held at 1100°C or 1150°C for 200 hrs.

The absorption in the visible and IR was studied by a variation of the PCI technique that takes advantage of two pump beams, for example, blue-green and infrared, that are crossed with a wider probe beam inside the sample (Figure 1).

Different photothermal techniques have been used previously as a sensitive tool for measurement of light absorption, mainly in chemical analysis of gases and liquids.⁵ The technique used in this work is a modification of the thermal lensing technique

* Correspondence: E-mail: alexei@loki.stanford.edu; Telephone : 650 723 0464; Fax 650 723 2666

UV and visible absorption in LiTaO₃

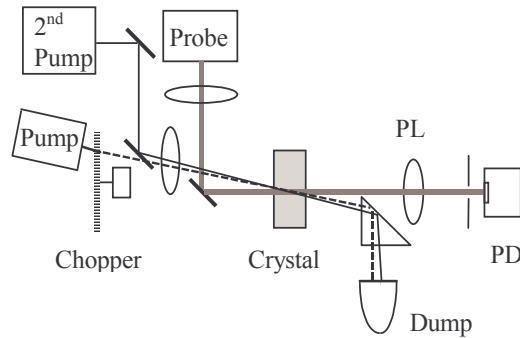


Figure 1. Crossed-beam setup for low absorption measurement. PL: projecting lens, PD: photodetector. Second pump is added whenever the influence of light with a different wavelength on absorption of the first pump is to be studied.

that also exploits the thermo-optic effect (index of refraction dependence on temperature: dn/dT). It differs from thermal lensing with its far-field detection scheme by utilizing a near-field detection scheme which approaches in sensitivity that of interferometric absorption measurement methods. With interferometric sensitivity, the PCI technique permits phase distortions, $\Delta\phi$, of the probe beam due to pump beam heating to be transformed into corresponding perturbations of the probe beam intensity, $\Delta I/I \approx \Delta\phi$. For materials with dn/dT around $10^{-5}/K$ and with pump power of 1W, this gives resolutions of ≤ 1 ppm in terms of the absorbed fraction of pump power. Details of this technique will be described elsewhere.⁴

With the PCI technique, fundamental material constants are in theory sufficient for calculating the absorption coefficients from the intensity perturbations detected. However, a 'standard' measurable by a direct loss method is desirable to avoid uncertainties in material constants. A Fe-doped LiTaO₃ crystal, with an absorption of 2.7 cm^{-1} at 1064 nm was used in this work to normalize the results in the low-loss near-IR to visible region.

For wavelengths near the absorption edge, where the absorptivity is sufficiently large, absorption spectra were obtained with conventional spectrophotometric techniques using a Hitachi model U4001 spectrophotometer. The effects of Fresnel reflections were eliminated by using samples of two different lengths.

3. RESULTS

3.1. UV residual absorption and impurities

Although its UV absorption edge goes farther in the UV than that of lithium niobate, an absorption band with a tail extending up to 400 nm limits the applications of LiTaO₃ in the short wavelength range.

The analysis of several different LiTaO₃ crystals, shown in Figure 2, indicates that some of them can exhibit extremely low absorption in the UV, and we have investigated which defects might be responsible for this effect.

The structure of LiTaO₃ is the same as that of LiNbO₃; several descriptions of the defect structure of LiNbO₃ are found in the literature.^{6,7} In LiNbO₃, two kinds of defects are dominating: electron traps and lithium vacancies. In the case of LiTaO₃, the electron traps can be intrinsic (tantalum ions on lithium sites at levels of a few %) or extrinsic (Fe^{3+} , Fe^{2+} or Cr^{3+} in ppm levels). These defects lead to chemical reduction of the material and can be responsible for bands of excess absorption.

Several experiments have been performed to identify the specific defects responsible for these bands. Heat-treatment studies have shown that the absorption around 300 nm, near the UV shoulder, is lower in reduced crystals (Figure 3).

While these observations are not consistent with Ta^{4+} centers, it has been shown that in LiTaO₃, Fe^{3+} exhibits an absorption band around 300 nm whereas the band for Fe^{2+} is around 400 nm.⁸ However, in our reduced crystals, the UV shoulder did not decrease enough for us to conclude that the absorption at 300 nm comes only from Fe^{3+} .

UV and visible absorption in LiTaO₃

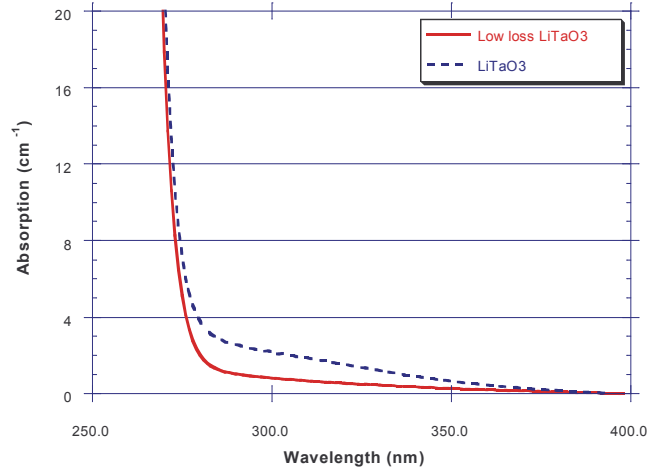


Figure 2: Absorption spectra for two different LiTaO₃ crystals.

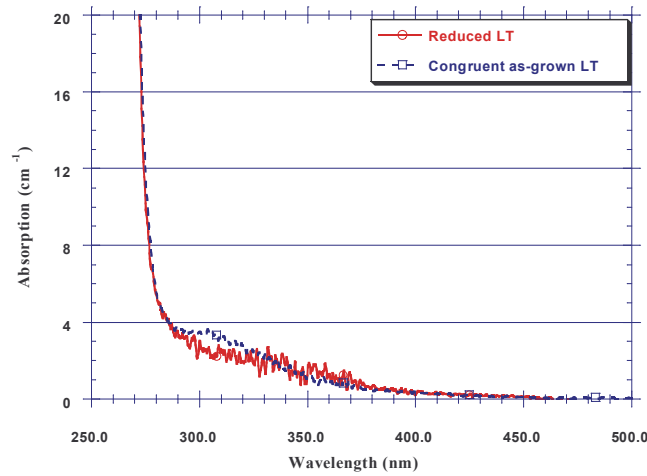


Figure 3: Effect of reduction on the UV absorption in LiTaO₃.

Ryba-Romanovski et al have studied the absorption of Cr³⁺ in LiTaO₃.⁹ Their results on absorption around 300 nm for a Cr³⁺ concentration of 500 ppm are consistent with the residual absorption we found in nominally undoped LiTaO₃, if we assume Cr³⁺ concentration of several ppm. Our absorption measurements performed on the LiTaO₃ cubes showed absorption bands at 462 nm and 650 nm which were attributed by Ryba-Romanovski, *op. cit.*, to Cr³⁺ (Figure 4). Moreover, Cr³⁺ is not easily reduced to Cr²⁺, which explains why we observed no changes resulting from the reducing heat-treatments.

The absorption band at 300 nm has been investigated in several LiTaO₃ crystals and the samples analyzed by glow discharge mass spectroscopy (GDMS). The results on absorption versus Cr³⁺ and Fe³⁺ concentrations are plotted in Figures 5 and 6.

UV and visible absorption in LiTaO₃

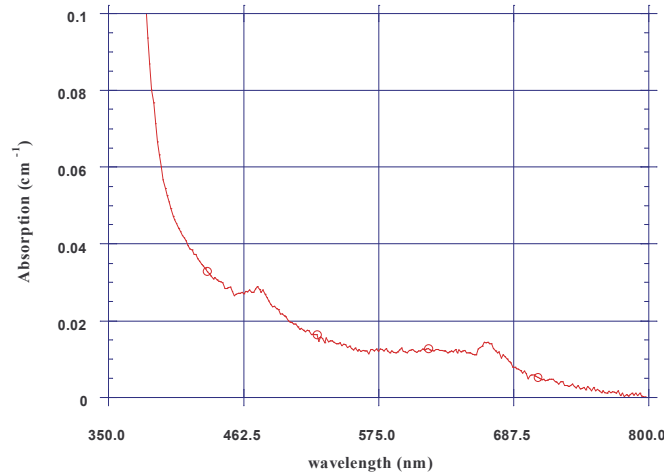


Figure 4: Absorption bands of Cr³⁺ in LiTaO₃.

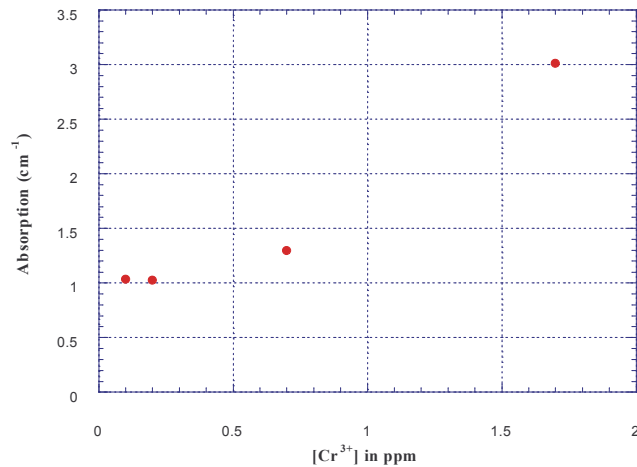


Figure 5: Effect of [Cr³⁺] on absorption at 300 nm.

The correlation between Fe³⁺ and Cr³⁺ concentrations in the crystals and the absorption band at 300 nm is clear. The lowest absorptions are found in crystals containing less than 0.5 ppm of Cr³⁺ and less than 1 ppm of Fe³⁺. It also appears that for concentrations below these levels, some residual absorption is still present. Whether this absorption is intrinsic to LiTaO₃ or comes from other impurities remains to be determined and further studies are in progress.

3.2. VTE results

In lithium niobate, one way to shift the UV edge farther into the UV is to increase the content of lithium in the crystal, moving it closer to stoichiometry than the lithium deficient composition of commercially available congruent crystals.¹⁰ We carried out similar lithium enrichment experiments on LiTaO₃ crystals using the VTE process. Figure 7 shows the result for a VTE experiment using LiTaO₃ with already low absorption in the UV. The UV edge shifted from ~280 nm to 260 nm and

UV and visible absorption in LiTaO₃

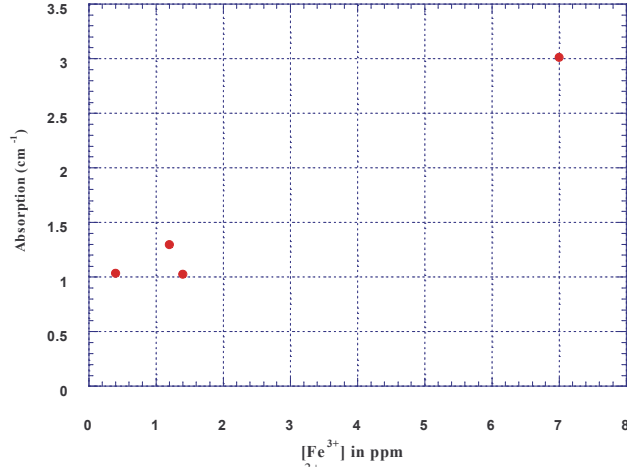


Figure 6: Effect of [Fe³⁺] on absorption at 300 nm.

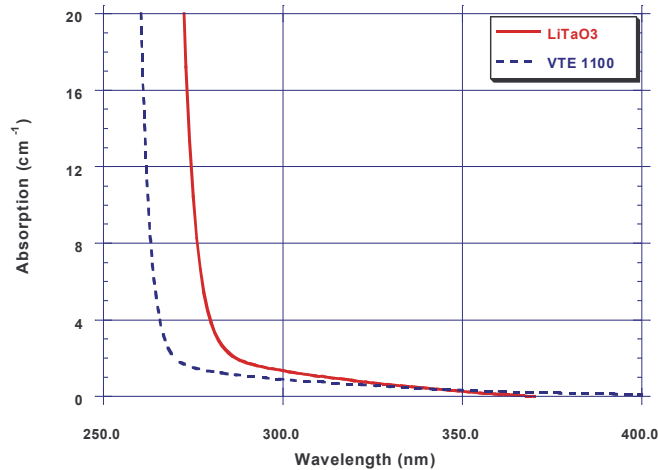


Figure 7: Effect on lithium enrichment on low-absorption LiTaO₃

there was no noticeable increase in the absorption in the UV. Another interesting property has been found on Li-enriched LiTaO₃; the coercive field for ferroelectric domain reversal drops from 21 kV/mm in congruent LiTaO₃ to 3kV/mm in Li-rich LiTaO₃, as happens in LiNbO₃.¹¹ In our Li-enriched LiTaO₃, these properties are independent of the VTE processing temperature over the range 1100°C to 1150°C, implying that there is little difference in composition between crystals processed in this temperature range. Experiments to explore effects of higher VTE processing temperatures are planned.

3.3. Green, IR absorption and GRIIRA

Data on different LiTaO₃ crystals are summarized in Table 1 together with characteristics of commercial optical grade, oxygen-annealed LiNbO₃. All data were obtained at room temperature with the pump propagating along the Z axis of the crystal. Other experiments verified that there is no strong difference in absorption for ordinary vs extraordinary polarizations. GRIIRA is characterized in Table 1 by the ratio of IR absorption in the presence of green light at a given power density to the IR absorption in the absence of green light.

UV and visible absorption in LiTaO₃

In Table 1, the values for photorefraction are estimates of the change in ordinary refractive index under the same conditions as for the GRIIRA measurements.

Table 1

Crystal	Absorption at 1064nm (cm ⁻¹)	absorption at 514nm (cm ⁻¹)	GRIIRA (13 kW/cm ²)	Photorefraction ($\Delta n_o \times 10^5$)
LiNbO ₃ , oxygen-annealed	0.0008	0.008	16 (13 kW/cm ²)	1.4
LiTaO ₃ #1, oxygen-annealed	0.004	0.006	< 0.02 (13 kW/cm ²)	< 0.1
LiTaO ₃ #1, reduced	0.09	0.1	3.5 (13 kW/cm ²)	1.0
LiTaO ₃ #16	0.0007	0.005	< 0.02 (13 kW/cm ²)	< 0.1
LiTaO ₃ #17	0.0017	0.007	< 0.02 (13 kW/cm ²)	< 0.1
LiTaO ₃ #59	0.003	0.032	1.7* (1.3 kW/cm ²)**	6.4
LiTaO ₃ #83	0.0012	0.011	1.14* (1.3 kW/cm ²)**	0.7
LiTaO ₃ #90	0.0015	0.016	1.45* (1.3 kW/cm ²)**	0.7

* GRIIRA suppressed by local bleaching as shown in Figure 8

** Electric discharges caused by photovoltaic fields at the surface of the sample distorted the response at higher green power levels.

In addition to GRIIRA, many LiTaO₃ crystals showed a strong local bleaching effect. A similar effect has been observed in periodically-poled lithium niobate at elevated temperatures.² The combination of these effects in LiTaO₃ is illustrated in Figure 8.

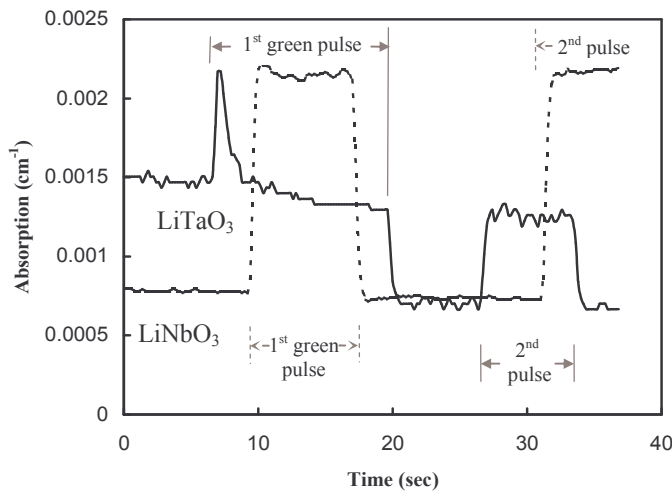


Figure 8. GRIIRA in LiTaO₃ #90 and oxygen-annealed LiNbO₃: the response of absorption at 1064 nm for green light at a power density of 1.3 kW/cm² which was applied as long pulses.

The sharp absorption peak observed in the LiTaO₃ crystal corresponds to the beginning of the first green pulse. The height of this peak was used to characterize GRIIRA as in Table 1. Bleaching is seen as a drop in the absorption signal below its initial level, which is seen after the end of the first pulse. The bleaching effect was observed to be local and persistent: the second green pulse resulted in a rectangular IR absorption response. In contrast, lithium niobate shows larger GRIIRA without any noticeable bleaching effect.

UV and visible absorption in LiTaO₃

The data in Table 1 show that high GRIIRA in LiTaO₃ is associated with large photorefraction and increased green absorption. On the other hand, the absorption near the UV edge is not correlated with these effects. For example, oxygen-annealed LiTaO₃ crystals displayed significant UV absorption shoulders while photorefraction was minimal and GRIIRA could not be observed up to the highest green power density used in our study, 13 kW/cm².

Unlike lithium niobate, LiTaO₃ crystals can be found that are free of GRIIRA. In these crystals photorefraction is much less than in LiNbO₃ and green absorption is comparable with or lower than that in LiNbO₃. One possible factor affecting both GRIIRA and photorefraction in some LiTaO₃ crystals may be the oxidation state of the material: moderate reduction has been found to increase GRIIRA and photorefraction dramatically (see second and third line in Table 1). In one literature model constructed to account for increased photorefraction and nonlinear green absorption in LiNbO₃ at high CW pump powers,¹² a combination of Fe impurities and Nb antisite defects (Nb in Li sites) was considered. If antisite niobium acts as a trap for electrons released from Fe³⁺, then the IR absorption should increase because the absorption band associated with isolated Nb⁴⁺ is in the near IR.⁶ By analogy with LiNbO₃, a mechanism that includes reduced tantalum may be operative in LiTaO₃.

The bleaching effect that accompanies GRIIRA in many LiTaO₃ crystals was observed to have different dynamics than the GRIIRA. The time constant for bleaching was generally longer than that for GRIIRA. This resulted in a sharp temporal increase of IR absorption, as shown in Fig.8. At the same time, the bleaching effect is stable, at least on the scale of minutes, while GRIIRA time constants are on the order of a few milliseconds. There seems to be no simple explanation for the local bleaching effect at this time. More complex defect models can probably be constructed to explain simultaneous GRIIRA, photorefraction and bleaching in LiTaO₃. However, additional data on the bleaching effect will be needed to understand its nature.

4. CONCLUSIONS

Residual UV absorption frequently observed in LiTaO₃ as a band extending from the band edge to 400 nm correlates with transition metal impurity content. Significantly lower UV absorption levels were detected in crystals with less than 0.5 ppm of Cr and less than 1 ppm of Fe. Other contributors to excess UV absorption are felt to be likely since little improvement in absorption was observed for Cr and Fe impurity concentrations below these levels.

GRIIRA in LiTaO₃ crystals is associated with large photorefraction and increased green absorption, but the absorption in the UV is uncorrelated with these effects. A combination of reduced tantalum (Ta⁴⁺) and Fe²⁺ impurities is one possible way to account for GRIIRA in LiTaO₃.

Unlike lithium niobate, LiTaO₃ crystals can be found which are apparently free of GRIIRA effect. In these crystals, photorefraction is much less than in LiNbO₃ and green absorption is comparable with or lower than that in LiNbO₃. This is a distinct advantage that suggests LiTaO₃ may be a more promising material for high average power devices operating in the blue-green spectral region.

As a result of VTE processing, the UV absorption edge shifted from ~280 nm down to 260 nm. If the UV absorption in the shoulder region can be shifted to shorter wavelengths yet, this would give an opportunity to extend the range for LiTaO₃-based devices further into the UV.

ACKNOWLEDGEMENTS

The authors wish to thank Crystal Technology, Inc. for providing the crystals and the setup for VTE experiments, and acknowledge useful discussions with Kenji Kitamura and Yasunori Furukawa.

REFERENCES

1. K. Mizuuchi, K. Yamamoto, and M. Kato, "Generation of ultraviolet light by frequency doubling of a red laser diode in a first-order periodically poled bulk LiTaO₃", *Appl. Phys. Lett.*, **70**, pp. 1201-1203, 1997.
2. R. G. Batchko, G. D. Miller, A. Alexandrovski, M. M. Fejer, and R. L. Byer, "Limitations of high-power visible wavelength periodically poled lithium niobate devices due to green-induced infrared absorption and thermal lensing," *Conference on Lasers and Electro-Optics*, 1998 OSA Technical Digest Series, **6**, pp. 75-76.

UV and visible absorption in LiTaO₃

3. P. F. Bordui, R. G. Norwood, D. H. Jundt, and M. M. Fejer, "Preparation and characterization of off-congruent lithium niobate crystals," *J. Appl. Phys.*, **71**, pp. 875-879, 1992.
4. A. Alexandrovski et al, to be published.
5. S. E. Bialkowski, *Photothermal Spectroscopy Methods for Chemical analysis*, Chemical analysis series, **134**, John Wiley & Sons, New York, 1996 .
6. O. F. Schirmer, O. Thiemann, and M. Wohlecke, "Defects in LiNbO₃ – I. Experimental aspects," *J. Phys. Chem. Solids*, **52**, pp. 185-200, 1991.
7. D. P. Birnie III, "Analysis of diffusion in lithium niobate," *J. Mater. Sci.*, **28**, pp. 302-315, 1993.
8. F. Nitanda, Y. Furukawa, S. Makio, M. Sato, and K. Ito, "Increased optical damage resistance and transparency in MgO-doped LiTaO₃ single crystals," *Jpn. J. Appl. Phys.*, **34**, pp. 1546-1564, 1995.
9. W. Ryba Romanowski, S. Golab, W. A. Pisarki, G. Dominiak-Dzik, M. N. Palatnikov, N. V. Sidorov, and V. T. Kalinnikov, "Influence of temperature on the optical properties of LiTaO₃:Cr," *Appl. Phys. Lett.*, **70**, pp. 2505-2506, 1997.
10. K. Polgar, A. Peter, L. Kovacs, G. Corraldi, and Zc. Szaller, "Growth of stoichiometric LiNbO₃ single crystals by the top seeded solution growth method," *J. Cryst. Growth*, **177**, 211-216 1997.
11. V. Gopalan, T. E. Mitchell, Y. Furukawa, and K. Kitamura, "The role of nonstoichiometry in 180o domain switching of LiNbO₃ crystals," *Appl. Phys. Lett.*, **72**, pp. 1981-1983, 1998.
12. F. Jermann and J. Otten, "Light-induced charge transport in LiNbO₃:Fe at high light intensities," *J. Opt .Soc. Am. B*, **10**, pp.2085-2092, 1993.